Transition-metal dichalcogenide bilayers: Switching materials for spintronic and valleytronic applications

Nourdine Zibouche,[1,2] Pier Philipsen,[2] Agnieszka Kuc,[1] and Thomas Heine[1,*]

[1]*School of Engineering and Science, Jacobs University Bremen, Campus Ring 1, 28759 Bremen, Germany*

[2]*Scientific Computing & Modelling NV, De Boelelaan 1083, 1081 HV Amsterdam, Netherlands*

(Received 16 April 2014; revised manuscript received 17 June 2014; published 22 September 2014)

We report that an external electric field applied normal to bilayers of transition-metal dichalcogenides TX_2 (T = Mo, W, X = S, Se) creates significant spin-orbit splittings and reduces the electronic band gap linearly with the field strength. Contrary to the TX_2 monolayers, spin-orbit splittings and valley polarization are absent in bilayers due to the presence of inversion symmetry. This symmetry can be broken by an electric field, and the spin-orbit splittings in the valence band quickly reach values similar to those in the monolayers (145 meV for MoS_2, ..., 418 meV for WSe_2) at saturation fields less than 500 mV Å^{-1}. The band gap closure results in a semiconductor-metal transition at field strength between 1.25 (WX_2) and 1.50 (MoX_2) V Å^{-1}. Thus, by using a gate voltage, the spin polarization can be switched on and off in TX_2 bilayers, thus activating them for spintronic and valleytronic applications.

DOI: 10.1103/PhysRevB.90.125440 PACS number(s): 73.61.Ga, 71.15.Mb, 71.20.Mq, 71.70.Ej

I. INTRODUCTION

Two-dimensional (2D) materials have been intensively investigated in the past few years for their applications in next-generation nanoelectronics, including spintronics [1] and valleytronics [2]. Transition-metal chalcogenides (TMCs) of the form TX_2 (T = Mo, W, X = Se, S) are of particular interest, as they have several interesting intrinsic properties, such as direct band gaps [3–5] or giant spin-orbit (SO) coupling (SOC) [6,7] in monolayered (ML) forms. The excellent electronic properties of TMCs have recently led to the production of the first nanoelectronic devices based on TMC-MLs, including thin-film transistors, logical circuits, amplifiers, and photodetectors [8–11]. It has also been reported that external stimuli, e.g., tensile strain [12–15], can strongly influence the electronic properties of TX_2 layers.

SOC is a relativistic effect that occurs for honeycomb 2D lattices with a broken inversion symmetry, such as in 2H TMC-MLs. Thus, for MoS_2, a giant spin-orbit-induced band splitting of ∼100 meV was reported from Raman experiments [7]. In agreement, from first principles the SO splitting in TX_2 MLs was calculated to be in the range 148–480 meV, with the limiting values for MoS_2 and WTe_2 MLs, respectively [6,16]. At the same time, TX_2 monolayers are very stable with respect to external electric fields, with a semiconductor-metal transition being reported for fields stronger than 4 V Å^{-1} [16]. In contrast, TX_2 bilayers have been found to be much more sensitive to external electric fields, with band gaps reducing linearly with respect to the external field [17,18].

It is very interesting to note that the SO splitting in TX_2 monolayers disappears nearly completely when going to bilayers (BLs). Indeed, in spintronic and valleytronic applications, it may be useful to have a material where the polarization can be switched on and off. This can be achieved if the inversion symmetry in the bilayer is broken by an external factor, most conveniently by an electric field normal to the lattice plane. It has already been suggested that the inversion symmetry can be broken in MoS_2 BLs through an external electric field applied normal to the planes, which leads to a potential difference between individual layers and allows control of valley polarization [19]. This effect should be even more pronounced for TX_2 materials that show stronger spin-orbit splittings in the monolayers, i.e., for WS_2 and WSe_2 [20]. Yuan *et al.* [21] have investigated the out-of-plane Zeeman-type spin polarization in the WSe_2 bilayer-based transistor using ionic-liquid-gate voltage. They have shown that such spin splitting can be induced and modulated by a perpendicular external electric field.

Therefore, we investigate here in detail the electronic structure of TX_2 bilayers as a function of an external electric field. We will show that similar SO splitting values as in the corresponding monolayers can also be achieved in TX_2 bilayers for a field strength in the range of 200–600 mV Å^{-1}. At this field strength, the materials are still semiconductors with appreciable band gaps of more than 500 meV. However, the band gap is a linear function of the applied electric field, and this provides additional means to tune the electronic properties. We have found that a field strength of about 1.5 V Å^{-1} is sufficient for the semiconductor-metal transition. This electric field strength can be achieved experimentally using, e.g., ionic liquid gating [22–24].

II. METHODS

All calculations were carried out using density-functional theory (DFT) with the Perdew-Burke-Ernzerhof (PBE) [25] exchange-correlation functional, with added London dispersion corrections as proposed by Grimme [26] and with Becke and Johnson damping as implemented in the ADF/BAND package [27,28]. Local basis functions [numerical and Slater-type basis functions of valence triple-zeta quality with one polarization function (TZP)] were adopted for all atom types, and the frozen-core approach (small core) was chosen. The k-point mesh over the Brillouin zone was sampled according to the Wiesenekker-Baerends scheme [29], where the integration parameter was set to 5, resulting in 15 k points in the irreducible

*t.heine@jacobs-university.de

 ©2014 American Physical Society

TABLE I. Calculated lattice parameters a (in Å) and the interlayer distances d measured between the metal planes (in Å) of all TMC bilayers at equilibrium. The corresponding values from Ref. [17] are given for comparison. Note that the authors used fixed experimental structures. The reoptimized values for the MoS_2 BL from Ref. [17] is given in parentheses.

	This work		Ref. [17]	
System	a	d	a	d
MoS_2	3.155	6.122	3.160 (3.199)	6.147 (6.180)
$MoSe_2$	3.268	6.425	3.299	6.469
WS_2	3.147	6.147	3.153	6.162
WSe_2	3.266	6.413	–	–

wedge. All TMC-BL structures (atomic positions and lattice vectors) are fully optimized, including scalar relativistic (SR) corrections, which are expressed by the zero-order regular approximation (ZORA) [30–33] to the Dirac equation. The implementation of the analytical gradients for SR-ZORA is based on a modification of the energy-gradient implementation in the nonrelativistic case. The difference from the latter arises in the calculation of the kinetic-energy gradients. Moreover, the full relativistic ZORA includes both the SR-ZORA and spin-orbit interactions [32,34]. The maximum gradient threshold was set to 10^{-4} hartree Å^{-1}. The lattice parameters and interlayer spacings are given in Table I. To obtain electronic structures (band structures and resulting electronic band gaps and spin-orbit splittings) at these optimized coordinates we performed full relativistic ZORA calculations [30,34]. At the same level of theory, the response to an external electric field normal to the lattice planes, ranging from 0.0 to 1.5 Å^{-1}, has been calculated. In ADF/BAND, the static electric field is homogeneous and is implemented along the z direction (i.e., the nonperiodic direction). It is important to note that neither the applied electric fields nor SOC influence the BL geometries.

III. RESULTS AND DISCUSSION

Calculated band structures of all studied TX_2 materials in the presence of external fields of 0.00, 0.60, and 1.55 V Å^{-1} are given in Fig. 1. In the absence of the electric field, the results are in close agreement with values reported previously

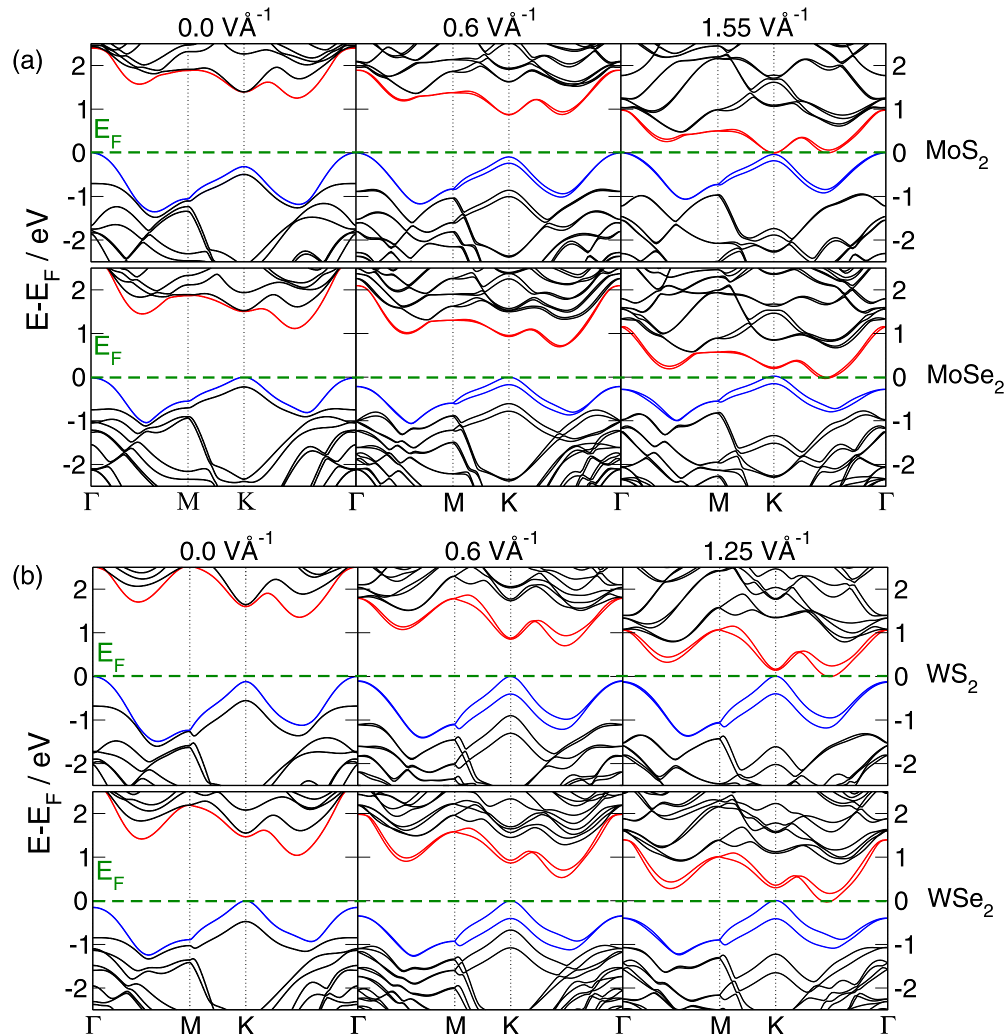

FIG. 1. (Color online) Calculated band structures of TX_2 bilayers under external electric field. The Fermi level E_F is shifted to the top of the valence band.

for the TX_2 bilayers [5]. All systems are indirect band gap semiconductors with band gaps Δ of 1.26, 1.14, 1.36, and 1.07 eV for MoS_2, $MoSe_2$, WS_2, and WSe_2, respectively. For the sulfide BLs, Kuc *et al.* [5] have obtained Δ of about 1.48 from the PBE nonrelativistic calculations, while Dashora *et al.* [35] calculated Δ of MoS_2 to be about 1.27 eV using the full-potential linearised augmented-plane wave approach with Wu and Cohen exchange-correlation potential. Using the local-density approximation within the plane-wave approach, Terrones *et al.* [36] obtained band gaps of BLs of 1.11, 1.05, 1.36, and 1.29 eV for MoS_2, $MoSe_2$, WS_2, and WSe_2, respectively. The valence-band maximum (VBM) is located at the high-symmetry K point of the Brillouin zone (BZ) for the selenides, while it is found at the Γ point for the sulfides. The conduction-band minimum (CBM) is always located at a low-symmetry point between K and Γ (Fig. 1, left panel).

The external electric field polarizes the electron density and thus introduces an anisotropy which creates an appreciable SOC. SO splitting is observed in both the conduction and valence bands, with the latter being more pronounced (Fig. 1, middle panel). The SO splitting of the VBM appears to have a natural saturation with a value very close to that of the respective monolayer. This saturation is reached already at the rather small inversion symmetry breaking caused by a field strength as small as 200 mV Å^{-1} (see Table II). At the same time, the valence bands are shifted closer to the Fermi level, and thus, the band gap is reduced. For larger fields of 1.55 V Å^{-1} for MoX_2 and 1.25 V Å^{-1} for WX_2, the conduction and valence bands cross the Fermi level, and the systems become metallic (Fig. 1, right panel).

Our results show an appreciable Stark effect [37]; that is, due to SOC in an external electric field, spin splittings are induced in the electronic bands in the structurally centrosymmetric BLs. The external field polarizes the electrons in the BLs in such a way that the inversion symmetry is broken. This causes SO splittings in a way similar to that in the monolayers. Figure 2 shows the spin-splitting values Δ_{SO} at the K point for the whole range of applied field strengths. At zero field strength, the spin-orbit splitting in BLs is zero; however, for very weak fields the situation drastically changes. In the VBM, Δ_{SO} reaches its maximum of 170 meV (420 meV) for molybdenum (tungsten) dichalcogenides and remains unchanged for the whole range of applied field strengths (see Table II). This is in close agreement with Δ_{SO} reported by Ramasubramaniam *et al.* [17] for MoS_2 BLs; they reported $\Delta_{SO} = 140$ meV at a similar field strength. In the

TABLE II. The calculated band gap values at zero electric field $\Delta_{E=0}$, the critical electric fields for the semiconductor-metal transition E_{crit}, the spin-orbit splitting values at saturation (Δ_{SO}^{sat}) and at an electric field of 200 mV Å^{-1} ($\Delta_{SO}^{E=0.2}$), and the electric field values for SO saturation of 90% $E_{SO=90\%}$.

System	$\Delta_{E=0}$ (eV)	E_{crit} (V Å^{-1})	Δ_{SO}^{sat} (meV)	$\Delta_{SO}^{E=0.2}$ (meV)	$E_{SO=90\%}$ (V Å^{-1})
MoS_2	1.26	1.50	145	136	0.2
$MoSe_2$	1.14	1.50	173	137	0.4
WS_2	1.36	1.25	404	335	0.4
WSe_2	1.07	1.25	418	212	0.6

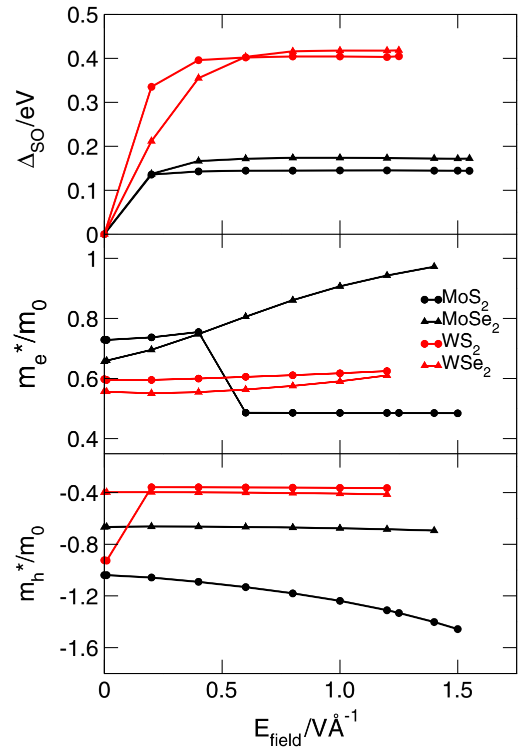

FIG. 2. (Color online) Calculated valence-band spin-orbit splitting values (Δ_{SO}) and the effective masses of electrons and holes (m_e^* and m_h^*) of the TX_2 bilayers as a function of applied perpendicular electric field. Δ_{SO} is calculated at the K point, while the effective masses are obtained from the valence-band maxima and conduction-band minima for the holes and electrons, respectively. Note the negative scale on the y axis for hole effective masses that arises from the curvature of the valence-band maximum.

CBM of all TX_2 bilayers we have obtained nonzero Δ_{SO}; however, the values are smaller than those in the VBM. The much larger Δ_{SO} found for the WX_2 BLs are due to the heavier tungsten atoms. Small variations in Δ_{SO} due to atom-mass differences can be observed between selenides and sulfides, but they do not exceed 30 meV. Incidentally, the calculated spin-orbit splittings of the valence bands almost coincide with the values known for the corresponding TX_2 monolayers [6,7,16].

Interestingly, the effect of the external electric field on the mobilities of electrons and holes is quite different in the four TX_2 structures (Fig. 2). For MoS_2, effective hole masses m_h^* increase with the applied field due to flattening of the bands. As the CBM moves already at a small applied field (400 mV Å^{-1}) to the K point in the BZ, we observe a discontinuity in the effective electron masses m_e^* and assume a strong increase in electron mobility for this system. In $MoSe_2$, m_e^* increase with applied electric field, while m_h^* remain stable. Both tungsten dichalcogenides show stable m_e^* with respect to the external field. The same is true for m_h^* in WSe_2, while for WS_2 VBM changes from Γ to K in the BZ at fields higher than 200 mV Å^{-1}. In general, the effective masses are smaller for the tungsten compounds, with the exception of m_e^* for MoS_2 at high external fields.

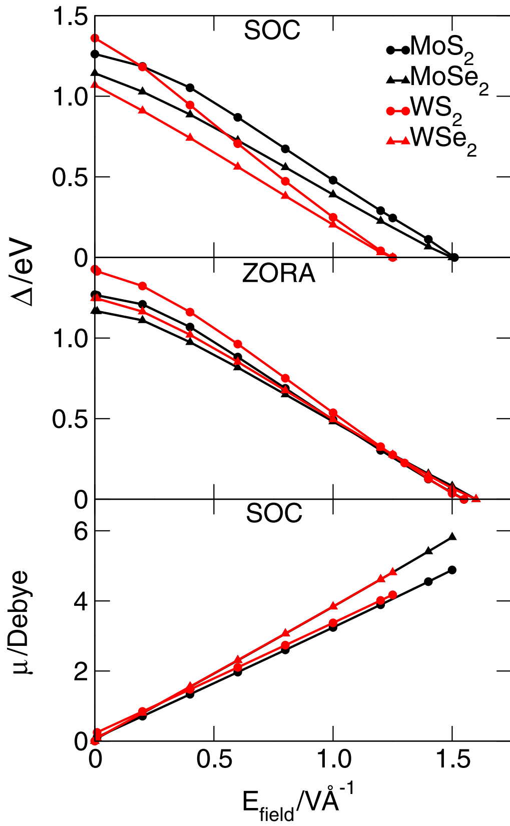

FIG. 3. (Color online) Calculated electronic band gaps Δ and dipole moments μ of TX_2 bilayers as a function of applied perpendicular electric field. For comparison, Δ is reported for both SOC and ZORA calculations.

Two reports have already discussed an interesting evolution of the electronic band gap Δ as a function of the external field. Ramasubramaniam and coworkers [17] have shown that the electronic structure of MoX_2 ($X = S, Se, Te$) and WS_2 bilayers can be influenced by a perpendicular electric field. Their first-principles-based plane-wave simulations suggested that the electronic band gaps decrease linearly with the field strength, resulting in a semiconductor-metal transition for relatively small electric fields in the range of 200–300 mV Å^{-1}. These values have been challenged by Liu *et al.* [18], who reassessed these studies while focusing on one material (MoS_2) but considered different stacking configurations of molybdenum and sulfur atoms in the 2D layers. They reported that the electric field strength at which the band gap closes is significantly higher, between 1.0 and 1.5 V Å^{-1}, and suggested that the smaller values reported by Ramasubramaniam *et al.* [17] are caused by applying inappropriate constrains to the symmetry of the bilayer structures. However, Liu *et al.* focused on MoS_2 and its band gap without considering SO effects.

We have calculated the band gap Δ evolution with respect to the applied electric field strength for various TX_2 bilayers. Our results, obtained using explicit two-dimensional boundary conditions and thus avoiding possible artifacts due to periodicity in the direction normal to the layers, support the assessment of Liu *et al.* [18]: as shown in Fig. 3, the electronic band gaps reduce nearly linearly with applied field strengths, and the materials undergo a semiconductor-metal transition at 1.25 and 1.50 V Å^{-1} for WX_2 and MoX_2 BLs, respectively.

In more detail, our calculations agree well with other first-principles simulations where available. For example, at equilibrium, the MoS_2 BL is an indirect band gap semiconductor with Δ of 1.26 eV, in excellent agreement with the calculations of Ramasubramaniam *et al.* [17], who obtained 1.26 eV from the fixed experimental structures and 1.13 eV from structures optimized at the PBE functional with Grimme's semiempirical dispersion correction level. Those values correspond, however, to a different system of higher symmetry, and the smaller Δ values of the optimized structures of Ramasubramaniam *et al.* [17] are due to the elongated in-plane lattice vectors (see

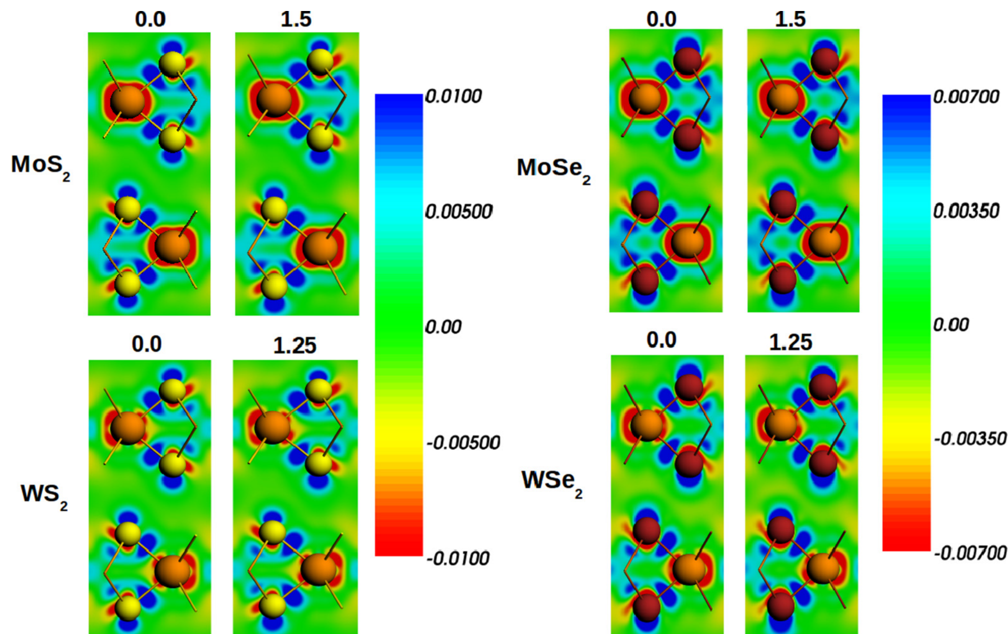

FIG. 4. (Color online) Density difference maps calculated at zero and critical electric field strengths for the (left) TS_2 and (right) TSe_2 bilayers.

also Table I). This is consistent with our earlier work, where we showed that under tensile strain the band gap reduces almost linearly [14,15]. For the MoS_2 BL, Liu *et al.* [18] obtained a 1.09 eV band gap at the local-density-approximation level and a semiconductor-metal transition at an external field of $\sim$1.5 eV Å^{-1}, which is in close agreement with our results but three times larger than those reported by Ramasubramaniam *et al.* [17].

Our calculations further show that W-based systems close their band gaps at lower fields than their Mo-based counterparts. This difference is not captured without considering SO effects. WS_2 bilayers show the strongest band gap dependence on the external field. This system inherently has the largest band gap among all the studied systems, but its Δ decreases most rapidly with the applied field.

The polarization of the lattice planes is reflected by the induced dipole moments μ (see Fig. 3) and the electron density distribution plotted in Fig. 4. Dipole moments are significantly larger than those for the respective monolayers [16]. Within the field strengths applied in this work, the dipole moments for all systems increase linearly with the applied field. For critical field strengths, μ of sulfide BLs are smaller than those for selenides by $\sim$1.0 D.

IV. CONCLUSION

In summary, spin splitting due to the spin-orbit coupling can be induced in centrosymmetric transition-metal dichalcogenide bilayers by an external electric field applied perpendicular to the layers. The necessary electric fields have a magnitude that can be reached by applying a gate voltage. Thus, the electronic properties of TX_2 bilayers can be controlled in a simpler and more effective way compared to mechanical deformations.

The electric field causes polarization of individual layers in such a way that the inversion symmetry is broken. As a result, band structures are strongly altered, and the spin splitting due to the Stark effect can be enhanced in the valence and conduction bands. The resulting materials are spin- and valley-polarized semiconductors. In addition, the electronic band gaps of all TX_2 bilayers reduce linearly with applied field, and eventually, these systems undergo a transition from a semiconducting to a metallic phase at field strengths of 1.2 and 1.5 V Å^{-1} for W- and Mo-based TX_2 bilayers, respectively. As such field strengths could be realized in practical nanoelectronic devices, we expect very interesting application possibilities in the emerging field of spintronics and valleytronics.

ACKNOWLEDGMENTS

Financial support from Deutsche Forschungsgemeinschaft (DFG, Grant No. HE 3543/17-1) and the European Commission through the Initial Training Network (ITN) MoWSeS (GA 317451) and the Industrial Academic Partnership Pathways (IAPP) QUASINANO (GA 251149) is acknowledged.

[1] I. Zutic, J. Fabian, and S. Das Sarma, Rev. Mod. Phys. **76**, 323 (2004).
[2] T. Cao, G. Wang, W. Han, H. Ye, C. Zhu, J. Shi, Q. Niu, P. Tan, E. Wang, B. Liu, and J. Feng, Nat. Commun. **3**, 887 (2012).
[3] K. F. Mak, C. Lee, J. Hone, J. Shan, and T. F. Heinz, Phys. Rev. Lett. **105**, 136805 (2010).
[4] A. Splendiani, L. Sun, Y. B. Zhang, T. S. Li, J. Kim, C. Y. Chim, G. Galli, and F. Wang, Nano Lett. **10**, 1271 (2010).
[5] A. Kuc, N. Zibouche, and T. Heine, Phys. Rev. B **83**, 245213 (2011).
[6] Z. Y. Zhu, Y. C. Cheng, and U. Schwingenschlögl, Phys. Rev. B **84**, 153402 (2011).
[7] L. Sun, J. Yan, D. Zhan, L. Liu, H. Hu, H. Li, B. K. Tay, J.-L. Kuo, C.-C. Huang, D. W. Hewak, P. S. Lee, and Z. X. Shen, Phys. Rev. Lett. **111**, 126801 (2013).
[8] H. Wang, L. Yu, Y.-H. Lee, Y. Shi, A. Hsu, M. L. Chin, L.-J. Li, M. Dubey, J. G. Kong, and T. Palacios, Nano Lett. **12**, 4674 (2012).
[9] O. Lopez-Sanchez, D. Lembke, M. Kayci, A. Radenovic, and A. Kis, Nat. Nanotechnol. **8**, 497 (2013).
[10] B. Radisavljevic, A. Radenovic, J. Brivio, V. Giacometti, and A. Kis, Nat. Nanotechnol. **6**, 147 (2011).
[11] B. Radisavljevic, M. B. Whitwick, and A. Kis, Appl. Phys. Lett. **101**, 043103 (2012).
[12] W. S. Yun, S. W. Han, S. C. Hong, I. G. Kim, and J. D. Lee, Phys. Rev. B **85**, 033305 (2012).
[13] E. Scalise, M. Houssa, G. Pourtois, V. Afanas'ev, and A. Stesmans, Nano Res. **5**, 43 (2012).
[14] M. Ghorbani-Asl, N. Zibouche, M. Wahiduzzaman, A. F. Oliveira, A. Kuc, and T. Heine, Sci. Rep. **3**, 2961 (2013).
[15] M. Ghorbani-Asl, S. Borini, A. Kuc, and T. Heine, Phys. Rev. B **87**, 235434 (2013).
[16] N. Zibouche, P. Philipsen, T. Heine, and A. Kuc, Phys. Chem. Chem. Phys. **16**, 11251 (2014).
[17] A. Ramasubramaniam, D. Naveh, and E. Towe, Phys. Rev. B **84**, 205325 (2011).
[18] Q. Liu, L. Li, Y. Li, Z. Gao, Z. Chen, and J. Lu, J. Phys. Chem. C **116**, 21556 (2012).
[19] S. Wu, J. S. Ross, G.-B. Liu, G. Aivazian, A. Jones, Z. Fei, W. Zhu, D. Xiao, W. Yao, D. Cobden, and X. Xu, Nat. Phys. **9**, 149 (2013).
[20] X. Xu, W. Yao, D. Xiao, and T. F. Heinz, Nat. Phys. **10**, 343 (2014).
[21] H. Yuan, M. S. Bahramy, K. Morimoto, S. Wu, K. Nomura, B.-J. Yang, H. Shimotani, R. Suzuki, M. Toh, C. Kloc, X. Xu, R. Arita, N. Nagaosa, and Y. Iwasa, Nat. Phys. **9**, 563 (2013).
[22] J. T. Ye, Y. J. Zhang, R. Akashi, M. S. Bahramy, R. Arita, and Y. Iwasa, Science **338**, 1193 (2012).
[23] J. Ye, Y. Zhang, Y. Kasahara, and Y. Iwasa, Eur. Phys. J. Spec. Top. **222**, 1185 (2013).
[24] Y. J. Zhang, J. T. Ye, Y. Yomogida, T. Takenobu, and Y. Iwasa, Nano Lett. **13**, 3023 (2013).
[25] J. P. Perdew, K. Burke, and M. Ernzerhof, Phys. Rev. Lett. **77**, 3865 (1996).

[26] S. Grimme, J. Comput. Chem. **27**, 1787 (2006).
[27] G. te Velde and E. J. Baerends, Phys. Rev. B **44**, 7888 (1991).
[28] P. H. T. Philipsen, G. te Velde, E. J. Bearends, J. A. Berger, P. L. de Boeij, J. A. Groenveld, E. S. Kadantsev, R. Klooster, F. Kootstra, P. Romaniello, D. G. Skachkov, J. G. Snijders, G. Wiesnekker, and T. Ziegler, BAND2012, SCM, Theoretical Chemistry, Vrije Universiteit, Amsterdam, 2012, http://www.scm.com.
[29] G. Wiesenekker and E. J. Baerends, J. Phys. Condens. Matter **3**, 6721 (1991).
[30] P. H. T. Philipsen, E. van Lenthe, J. G. Snijders, and E. J. Baerends, Phys. Rev. B **56**, 13556 (1997).
[31] E. van Lenthe, E. J. Baerends, and J. G. Snijders, J. Chem. Phys. **99**, 4597 (1993).
[32] E. van Lenthe, A. Ehlers, and E.-J. Baerends, J. Chem. Phys. **110**, 8943 (1999).
[33] M. Filatov and D. Cremer, Mol. Phys. **101**, 2295 (2003), .
[34] E. van Lenthe, J. G. Snijders, and E. J. Baerends, J. Chem. Phys. **105**, 6505 (1996).
[35] A. Dashora, U. Ahuja, and K. Venugopalan, Comput. Mater. Sci. **69**, 216 (2013).
[36] H. Terrones, F. Lopez-Urias, and M. Terrones, Sci. Rep. **3**, 1549 (2013).
[37] J. Stark, Ann. Phys. (Berlin, Ger.) **353**, 193 (1915).